Discharge and sedimentation periodicities in small sized watersheds

Ranjan S. Muttiah[a,*,1], R. Daren Harmel[b], Clarence W. Richardson[b]

[a]*Texas Agricultural Experiment Station, 808 East Blackland Road, Temple, Texas 76502, United States*
[b]*USDA-ARS, Grassland Soil and Water Laboratory, 808 East Blackland Road, Temple, Texas 76502, United States*

Abstract

We used wavelets to analyze the measured discharge and sedimentation during 2001 from the nested Agricultural Research Service watershed in Riesel Texas. Periodicities from wavelet spectra were interpreted in terms of experiments conducted on granular particle systems. Our time series analysis suggested (1) terracing in small watersheds can change nature of turbulence to an extent that sedimentation bears no relationship to flows; (2) fragmentation and shifting of sedimentation periodicities relative to discharge are common in upland erosion; and (3) sedimentation in transport flows displayed additional complex behavior involving recombination of discharge periodicities.
© 2005 Elsevier B.V. All rights reserved.

Keywords: Wavelets; Eddy bursts; Upland erosion; Transport flow; Fragmentation of periodicity; Shifting of periodicity

1. Introduction

Sedimentation at watershed scales is often estimated from water discharge measured at outlets. In such approaches, the rainfall erosivity index (EI index) in the soil loss

* Corresponding author. Tel.: +1 254 774 6103; fax: +1 254 770 6561.
  E-mail addresses: r.muttiah@tcu.edu (R.S. Muttiah), dharmel@spa.ars.usda.gov (R.D. Harmel), crichardson@spa.ars.usda.gov (C.W. Richardson).
  [1] Present Address: Center for GIS & Remote Sensing, Department of Geology, TCU, Fort Worth, TX 76129, United States.

equation is replaced by some estimate of stream power (Williams, 1975). In this paper, modern time series analysis using wavelets was performed on sub-hourly measurements to determine scale-time (periodicity) relationship between sediment loss (sedimentation) and discharge in small watersheds ranging in size from a few to over a hundred hectares. Wavelet transforms generate periodicity from time series similar in nature to the short-time Fourier transform but using localized basis functions (Kaiser, 1999). While we present results on the periodicities for water discharge and sediment, wavelets may also be suitable for determining relative contribution of suspended and bed load transport to dynamic sedimentation (//www.brc.tamus.edu/blackland/staff/muttiah/addinfo.html).

An important reason for application of wavelets in signal processing of environmental data is that wavelet transforms can mathematically describe non-periodic signals. Smith et al. (1998) applied a Mexican hat wavelet transform to classify basin discharge data according to hydro-climatic regions of the United States. When Ababou and Mangin (2001) compared spectral and correlation analysis with wavelet transforms of discharge from a karst watershed in France, they found that rainfall and runoff processes had different time scales with significant half-year and one-year components. Kumar (2000) found seasonal and high variability modes when wavelets were applied on the rotated principal components of flow. Nakken (1999) utilized wavelets to differentiate natural climate variability from non-stationary trends in runoff for the Upper Began River catchment in central western New South Wales, Australia. For the time period between 1911 and 1996, climate induced catchment response ranged from 27 to 32 months. Cahill (2002) used a wavelet-based test to detect changes in time series variance for 12 rivers in the United States between 1954 and 1999, while Whitcher et al. (2002) used Discrete Wavelet Transforms (DWT) to test for homogeneity of variance for a time series with long term memory. The changes in variances showed similarities at the larger ("stretched") wavelet scales. Kumar and Foufoula-Georgiou (1993) decomposed a squall line over Norman, Oklahoma using a Haar wavelet transform and determined that the average field (A) was related to external atmospheric forcing, and the fluctuation fields were related to internal storm dynamics. Wavelet analysis suggested that the general morphological characteristics of rainfall due to external atmospheric influences could be determined from the average field, and the internal fluctuations in rainfall were captured from the fluctuation fields. Chou and Wang (2002) re-parameterized the unit hydrograph with fewer wavelet coefficients and then convolved the hydrograph wavelet coefficients with effective rainfall to generate a one-step ahead runoff.

We were motivated to use wavelets to assess periodicity of time series since landscape and routed flow processes have characteristic periods (or frequencies) of occurrence. For instance, frequency of overland flow is responsive to time of concentration which represents the amount of time from soil saturation to initiation of runoff. Additionally, routed flows can occur at frequencies distinct from rainfall generated runoff pulses. Rainfall induced upland soil erosion can occur at a distinct frequency from that of transport in flowing rivers, both being dictated by the cascade and eddies in turbulent water. Our objectives were (1) analyze the periodicity in a year's worth (2001) of sub-
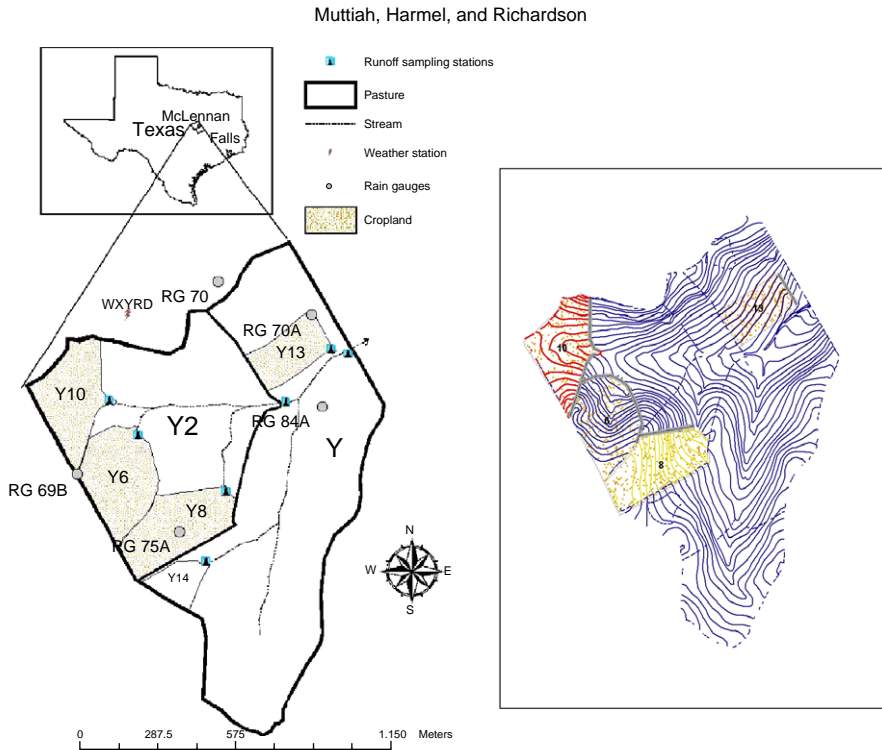
Muttiah, Harmel, and Richardson

Fig. 1. Layout of the Y sub-watersheds. The watershed is located in McLennan county in Central Texas. The contour lines on the right are at 1 ft intervals.

hourly discharge and sediment loss measurements in the nested Y watershed near Riesel Texas (Fig. 1) with complex wavelet transforms, and (2) determine the relationship between discharge and sedimentation periodicities.

2. Wavelet transforms

A continuous wavelet transform of a signal from some basic scale (j) to a coarser scale ($s = 2^j$) is generated from a mother wavelet by translation (τ) along the time axis according to (Burrus et al., 1998):

$$C(s,\tau) = s^{-1/2} \int f(t)\psi\left(\frac{t-\tau}{s}\right)dt \qquad (1)$$

where, Ψ is the wavelet and $f(t)$ is a continuous-time signal. The generated $C(s,\tau)$ for each scale and time of translation are known as "wavelet coefficients." The selection of the wavelet is determined by localization of signal energy in both scale and time. Generally, the wavelet basis function Ψ is generated from a scaling function φ such that Ψ is orthogonal to the scaling function and occupies the

Table 1
Sub-watershed attributes

Sub-watershed	Year	Month	Day	Management	Drainage area (ha.)	Bed slope %		Waterway length (m)	No. terrace flow paths	Flow length (m)	
						Channel	Terrace			Mean	S.D.
Y6	2001	4	19	Till with chisel plow	7.5	2.23	1.89	260	16	116	41
		4	26	Till with tandem disc							
		5	29	Till with sweep chisel							
		7	17	Till with sweep chisel							
		9	18	Pesticide application							
		9	26	Till with field cultivator							
		10	30	Till with field cultivator							
		11	2	Pesticide application							
Y8	2001	4	9	Shred with stalk cutter	8.42	2.21	1.31	215	10	202	33
		4	18	Till with chisel plow							
		4	25	Till with tandem disc							
		5	30	Till with sweep chisel							
		7	12	Fertilize							
		7	16	Till with sweep chisel							
		9	18	Pesticide application							
		9	27	Till with field cultivator							
		10	30	Till with field cultivator							
		11	2	Pesticide application							

Y10	2001	4	11	Shred with stalk cutter	6.6	2.02	1.86	300	9	143	50
		4	17	Till with chisel plow							
		4	24	Till with tandem disc							
		5	30	Till with sweep chisel							
		7	12	Fertilize							
		7	16	Till with sweep chisel							
		9	18	Pesticide application							
		9	27	Till with field cultivator							
		10	29	Till with field cultivator							
		11	2	Pesticide application							
Y13	2001	4	19	Till with chisel plow	4.61	1.82	1.92	150	5	275	8
		4	24	Till with tandem disc							
		6	1	Till with sweep chisel							
		7	13	Fertilize							
		7	16	Till with sweep chisel							
		9	26	Till with field cultivator							
		10	29	Till with field cultivator							
		11	2	Pesticide application							
Y2		N/A			54.7	1.56					
Y		N/A			125.1	1.84					

orthogonal complement spaces. In the case of discrete wavelet transforms, additional wavelets (beyond the first Ψ) in complimentary spaces are generated, and the signal $f(t)$ is decomposed on these wavelets (each wavelet is labeled by a level). When the convolution operation given by Eq. (1) for continuous wavelets is performed at each scale, $C(s,\tau)$ will yield higher values for those signal components that have the best spectral match with the dilated (or compressed) wavelet. When the wavelet function Ψ is complex, Eq. (1) returns information about the phase and amplitude of the similarity between the wavelet and the signal (Torrence and Compo, 1998). In frequency space, the time convolution Eq. (1) is a multiplication operation, and the wavelet spectrum is generated from Fourier transforms. We selected the complex Morlet wavelet transform from the wavelet analysis toolkit developed by Torrence and Compo (1998) since background red noise processes were separated from statistically significant features in the wavelet spectra.

3. Material and methods

The watershed Y with total drainage area of 125.1 ha is located near Riesel, Texas in the semi-arid Blackland Prairie physiographic province of Texas (Fig. 1). The study watershed is owned and operated by the USDA-ARS Grassland Soil and Water Research Laboratory in Temple, Texas. The Y6, Y8, and Y10 sub-watersheds drain into Y2, while sub-watersheds Y2 and Y13 drain to the outlet at Y. Contour terraces were established on Y6, Y8, Y10 in the 1940s, and in Y13 in the late 1960s. The cropped sub-watersheds had vegetated waterways that drained the fields shown as gray lines on the contour map in Fig. 1. The channels in the rest of the Y2 and Y watershed were vegetated with grass maintained by mowing or grazing. The terraces and waterways had variable slopes in the 1–2% range as shown in Table 1. The uniform soil throughout was Houston Black vertisol clay series (fine, smectitic, thermic, Udic Haplustert). Runoff water samples were taken with Chickasha-style samplers. These automated, mechanical samplers were activated with a float water level switch. Discrete samples were taken on variable time intervals with

Table 2

Measure schedule for runoff and sedimentation during storm events from the sub-watershed

Observation	Sub-watershed	Trigger (cfs)	Sampling interval upon trigger
Sediment	Y	5	1 sample at 5 min, then
	Y2	3	2 samples at 15 min, then
			3 samples at 30 min, then
			4 samples at 60 min, then
			14 samples at 120 min
	Y6	1	
	Y8	1	1 sample at 5 min, then
	Y10	1	4 samples at 15 min, then
	Y13	0.6	4 samples at 30 min, then
			4 samples at 60 min, then
			11 samples at 120 min

Table 3
Calculation of the vertical and horizontal eddy burst periods

	h (m)	W (m)	S	v^* $(= \sqrt{gSh})$ m/s	v (m/s)	T_v (s)	T_H (s)	T_H/T_v
Y6	0.23	8.23	0.0223	0.13		0.41	3.35	179	54
Y8	0.15	9.14	0.0221	0.18		0.54	1.65	151	91
Y10	0.30	5.0	0.0202	0.24		0.81	2.21	60	27
Y13	0.24	9.14	0.0182	0.21		0.68	2.10	120	57
Y2	0.33	8.22	0.0156	0.22		0.76	2.61	98	38
Y	0.60	11.0	0.0184	0.30		1.14	3.15	87	28
					Average		3.01	119.4	

h is depth of flow taken as bank full, W is flow width at bank full, v^* is friction velocity, T_v is period of vertical bursts given by 6 h/v from Yalin (1992), Eq. (2.6), T_H is period of horizontal bursts given by 9 W/v also from Yalin (1992), v is average flow velocity estimated using Eq. (1.28) in Yalin (1992) with k_s the surface roughness factor for the vegetated waterway taken as 40 based on Nezu and Nakagawa (1993).

more frequent samples taken on the rising leg of the hydrograph (see Table 2 for measurement schedule). Collected sediment was dried and weighed to determine sediment concentration. Flow rates were determined from the stage-discharge relationships for the flumes at each outlet.

Sub-daily flow and sedimentation measurement for the year 2001 were selected since land management on the cultivated sub-watersheds was kept the same (Table 1). The number of terraces, and flow length of terraces were determined from 1:40,000 (~1 m ground resolution) color infrared photography. Terrace and waterway slopes were determined from tape measurement during field visits. Sedimentation measurements were converted to units of kilograms, and discharge to units of m^3/s. Since flow and sediment measurements were based on intensity of rainfall events (with more sampling on rising limb of hydrograph), the data were "regularized" to 2 min intervals by interpolating between measurements with splines. Table 3 shows the calculated vertical and horizontal "eddy bursts" periods for each sub-watershed from Yalin (1992). The period of the vertical bursts was considerably shorter being less than 4 s, while the horizontal bursts were in the 60–180 s range. Thus, given the temporal limitations of our measurements, our sediment transport analysis is limited to being mostly governed by horizontal bursts.

Since the streams and therefore hydrologic measurements were intermittent, time periods when no measurements were made for lack of storms were ignored, and all measurements per sub-watershed were collated to one continuous time series. The *MATLAB* (version 6.5.0.180913a Release 13, *Mathworks*, Inc., Natick, Massachusetts) software package, and wavelet algorithms written by Torrence and Compo (1998) were used in our data analysis.

4. Results and discussion

Our interpretation of the periodicity plots for discharge and sedimentation was guided by experimental research on granular media by Jaeger and Nagel (1992), Jaeger et al. (1996), and Knight et al. (1993). Their relevant findings and our assumptions were as
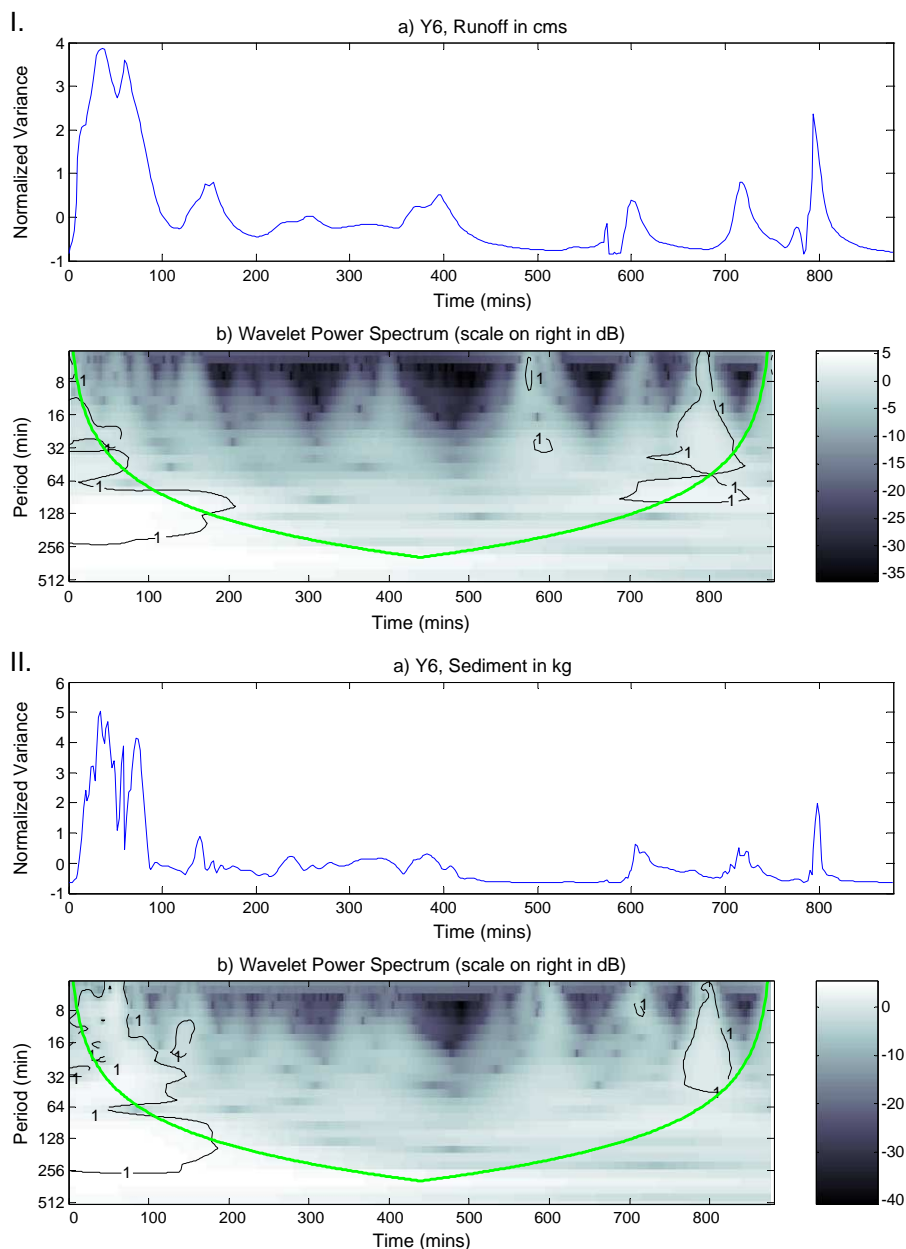
Fig. 2. Wavelet spectra for discharge (I) and sediment loss (II) from the Y6 sub-watershed during 2001. The normalized variance is based on 2 min interpolations of observed values. The thick line represents areas beyond which edge effects will lead to error, and the thin lines with label 1 represents areas that have 95% significance above a white noise process.
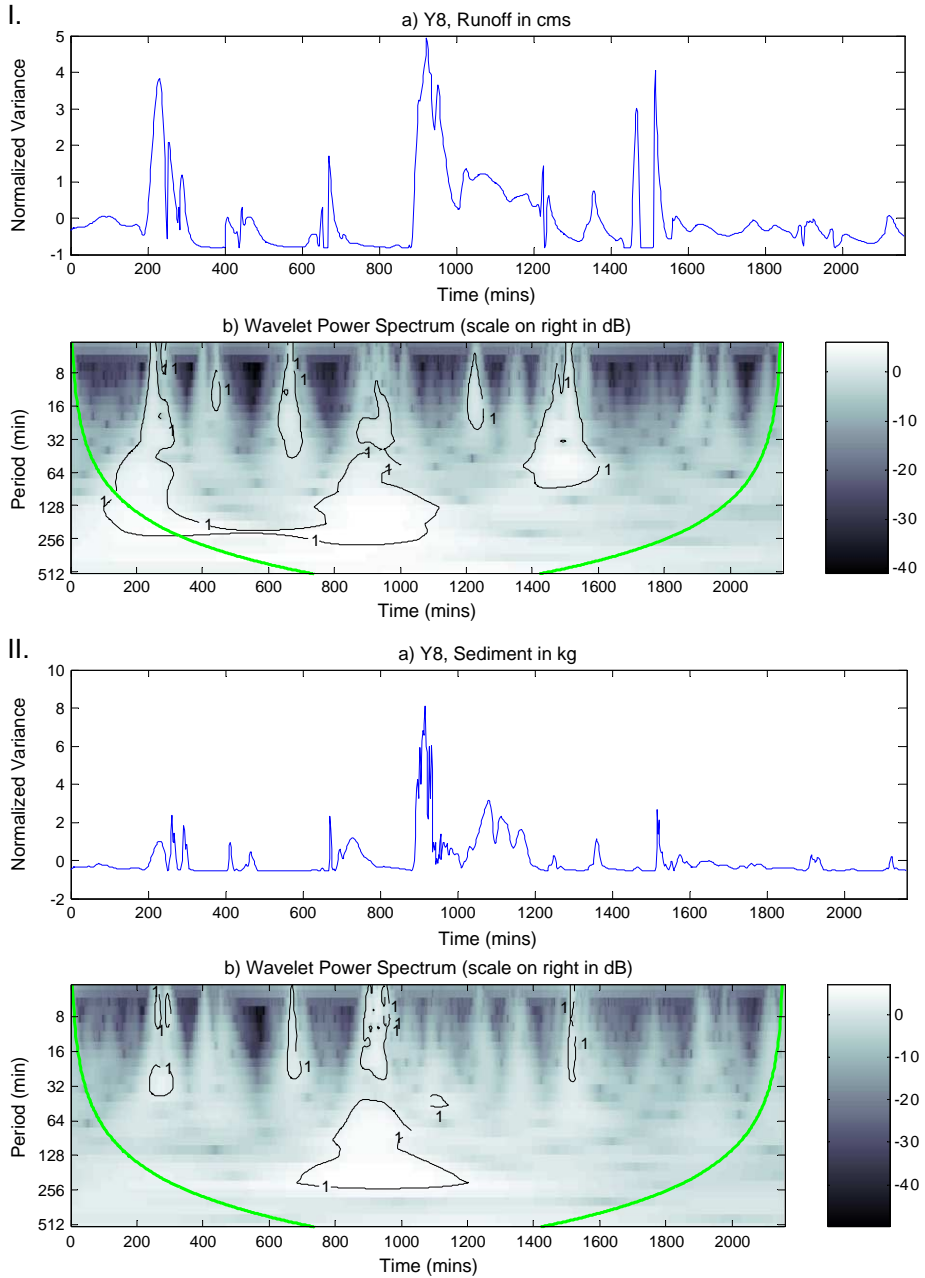
Fig. 3. Wavelet analysis for discharge and sedimentation from sub-watershed Y8.

follows: (1) if uniform sediment granules are externally forced into suspension with a sinusoid of frequency f, the suspended granules themselves form double ($2f$) and higher frequency patterns; (2) when granules collide, they form a clustered mass distribution upon
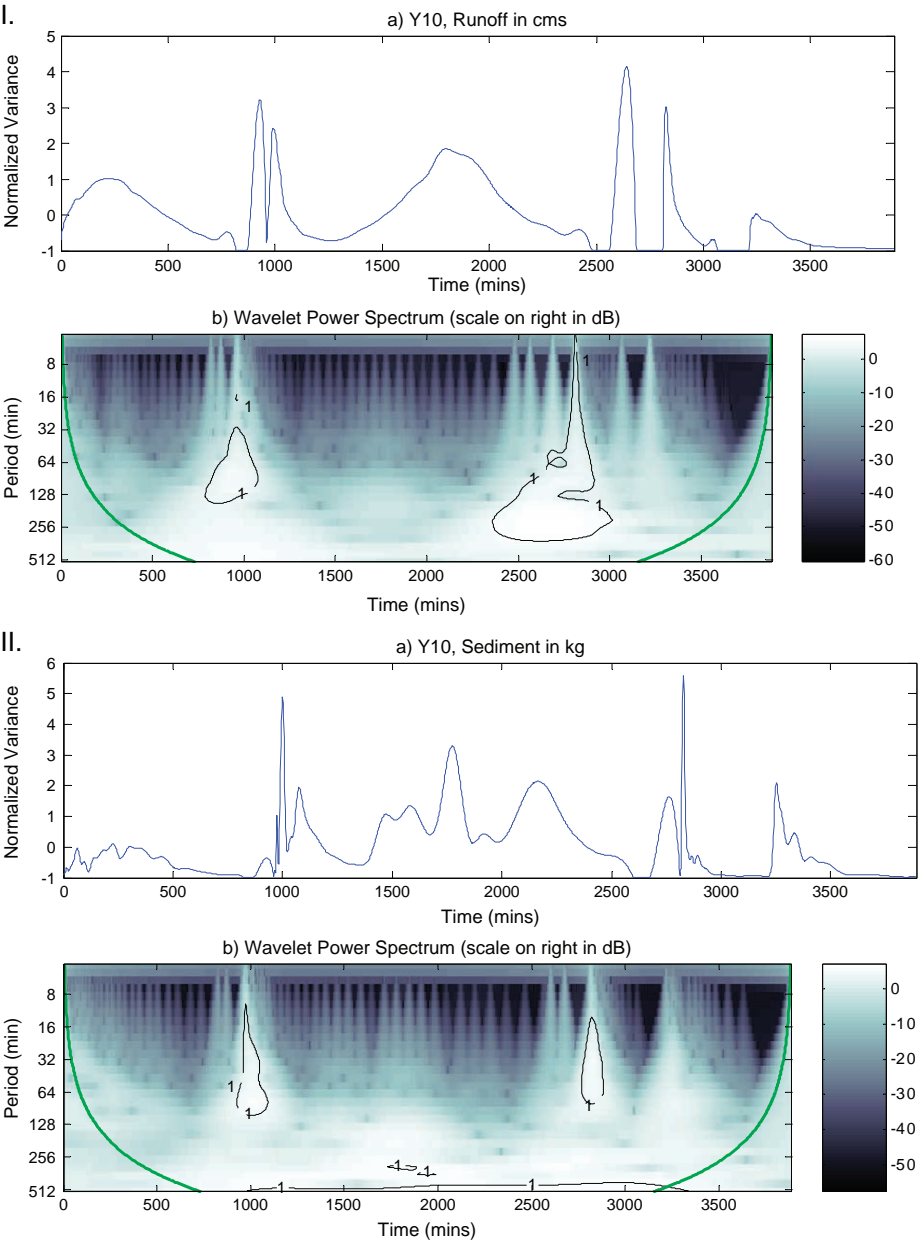
Fig. 4. Wavelet analysis for discharge and sedimentation from sub-watershed Y10.

settlement; and (3) while viscous to inertial interactions become important for low Bagnold numbes (<5,000), we assumed that periodicity of suspension/re-suspension of sediments was unaffected by viscous effects.

Figs. 2–4 show the wavelet power spectra generated by using complex Morlet wavelet on discharge and sedimentation in Y6, Y8, and Y10, respectively. These sub-watersheds cumulatively contribute flows to the Y2 outlet. The top graph in Fig. 2Ia is the normalized variance ($=[x - \mu]/\sigma^2$) for the discharge time series. The spectrum plot (Fig. 2Ib) depicts the periodicity in minutes on the abscissa, and time on the ordinate. The thick line on Fig. 2Ib represents the "cone-of-influence" area within which the "edge effects" due to padding the time series with zeros can be neglected (see Torrence and Compo, 1998 for details). The thin black lines (marked with label 1) enclose spectra with 95% probability of being above a lag-1 auto regressive red noise process. Fig. 2IIa and b contain the wavelet spectra for sedimentation in Y6. The standout features when comparing the discharge and sedimentation spectra for Y6, Y8, and Y10 are the shifting to lower periodicities, and fragmentation of periodicities for sedimentation. The sedimentation spectrum for Y10 also shows persistence of longer time periods in relation to discharge. For example, at time about 1000 min, the wavelet spectrum for Y8 discharge shows a continuous increase in periodicity, whereas the periodicity for sedimentation is fragmented into two distinct periodicities. Shifting from a continuum of periodicities to pulsed response is seen at about 200 min and 1500 min. The shifting and fragmentation in sedimentation spectra are attributed to the sub-harmonics of suspended particles when forced externally by the eddy bursts in turbulent flow regimes (assumption #1). The persistence of higher periodicities in the sediment spectra for Y10 may follow from assumptions #2 and #3), namely: sediment particles which have settled into clusters are re-suspended and track the longer term forcing created by overland flows through the time of concentration. The lack of spectral features in Y6 (Fig. 2) above the red noise may be from abatement of turbulent flows through the large number of terraces (Table 1).

Fig. 5 shows the discharge and sedimentation spectra for sub-watershed Y13. The fragmentary nature of sedimentation periodicity is clearly visible. Therefore, there is consistency in applying assumption #1 from Y8 to Y13. The absence of extended periods for Y13 (as was the case for Y10) may be due to the straight line terraces in Y13.

Fig. 6 for sub-watershed Y2 is interesting due to lack of clear fragmentation in sedimentation spectra relative to the discharge spectra. From Table 3, as the sub-watersheds get larger, the ratio between vertical and horizontal burst periods decreases, thereby necessitating increased temporal resolution in flow and sediment measurements. The low temporal resolution of our time series analysis (2 min) may be a contributing factor to absence of observed fragmentation in spectrum for sedimentation. However, it is noteworthy that there is correlation between discharge and sedimentation from small through to high periodicities in similarity to the Y13 spectra at $t = 2000$ min. We interpret this to mean that the closeness of Y13 to the Y2 outlet caused the sedimentation dynamics in Y2 to closely reflect that of Y13.

Wavelet analysis of measurements at Y (Fig. 7) shows fragmentation in periodicities for sedimentation relative to discharge at about 2000 min, shifting to lower periodicities at
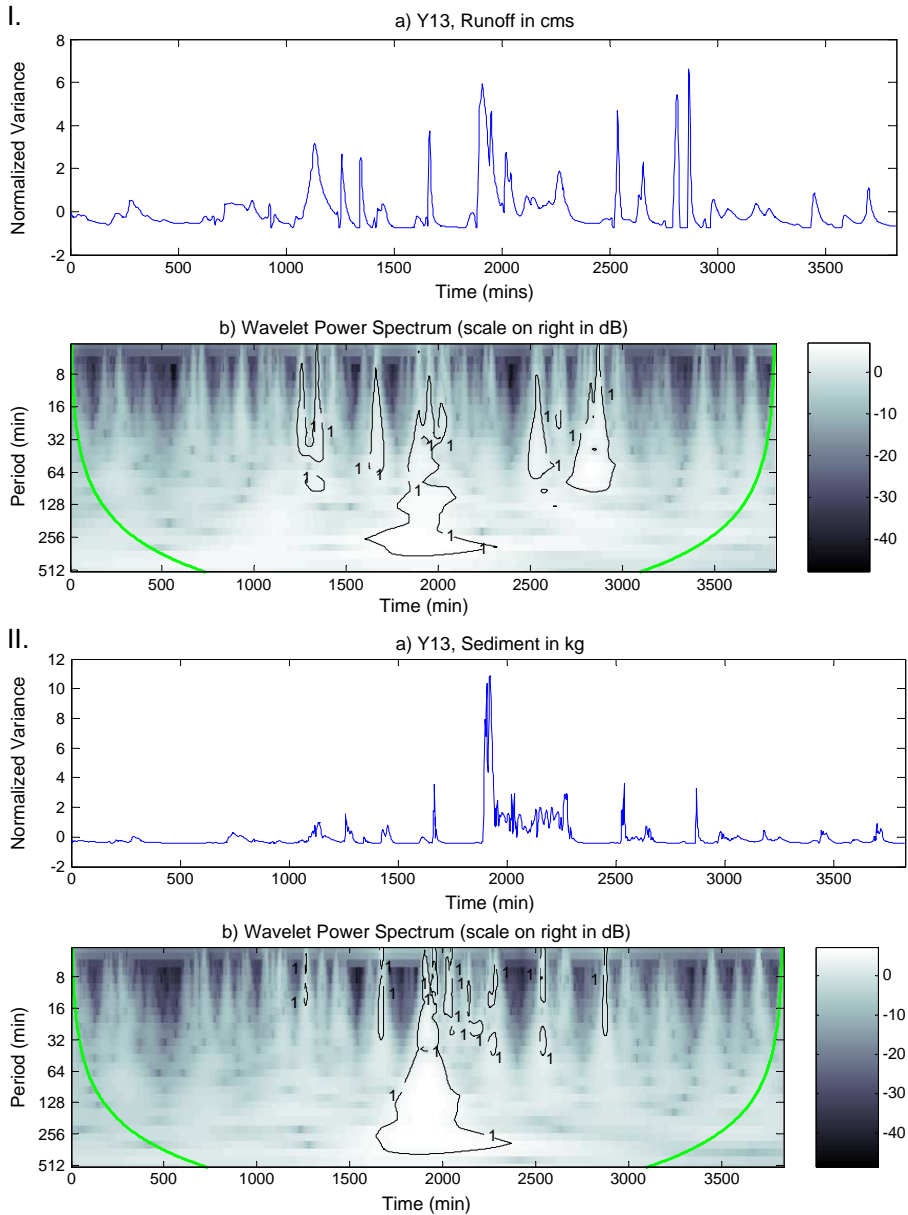
I.

II.

Fig. 5. Wavelet analysis for discharge and sedimentation from Y13.

3500–4000 min, and recombination of periodicities at about 3000 min. The fragmentation, recombination, and shifting are indicative of chaotic behavior of turbulence in routed flows even at the minute scale observation.
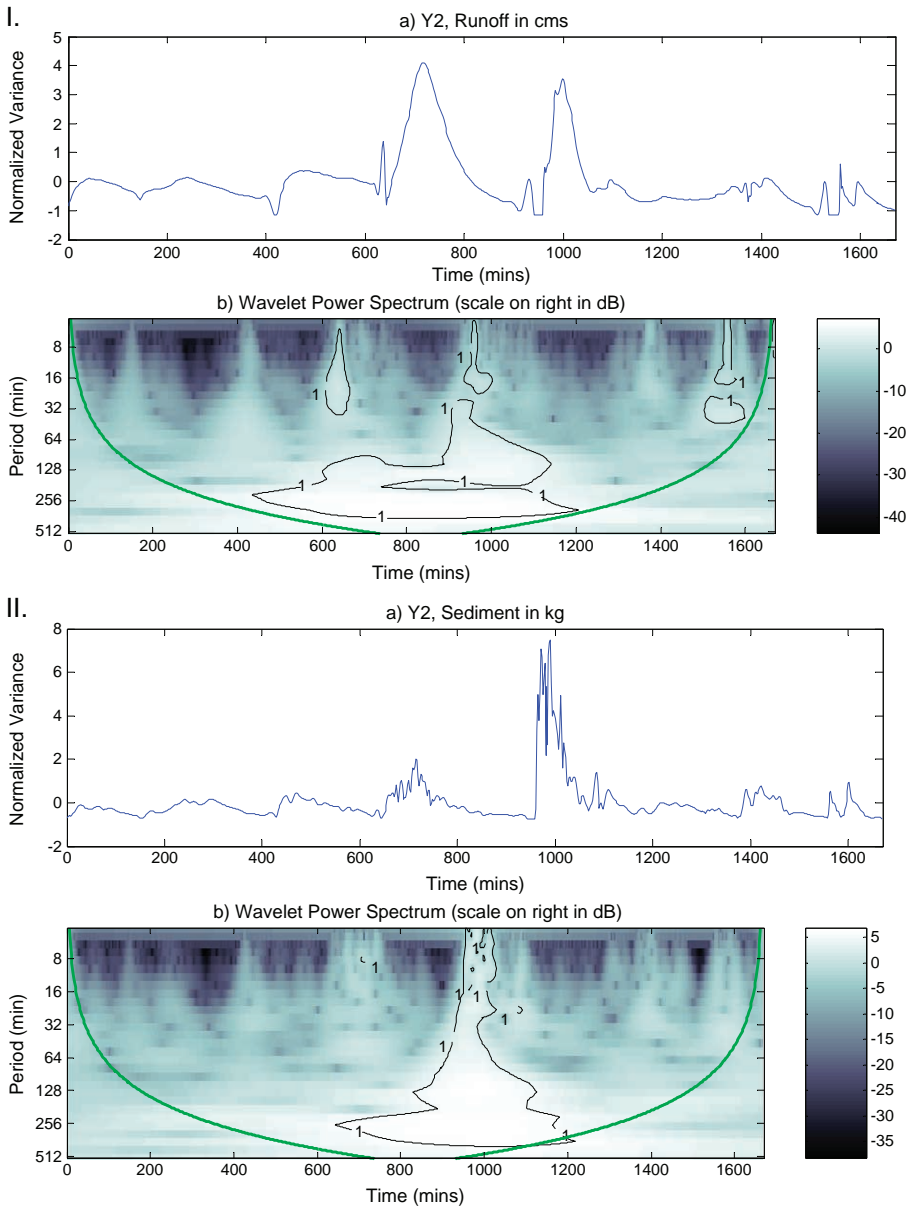
I.

a) Y2, Runoff in cms

b) Wavelet Power Spectrum (scale on right in dB)

II.

a) Y2, Sediment in kg

b) Wavelet Power Spectrum (scale on right in dB)

Fig. 6. Wavelet analysis for discharge and sedimentation from outlet at Y2.

Our analysis of discharge and sedimentation power spectra with wavelets suggests that small time step prediction (from hours to days) of sedimentation from discharge has to re-examine issues related to physical closeness of upland erosion areas to outlet, vertical and horizontal burst periods of turbulent flows, and the number of terraces that control upland
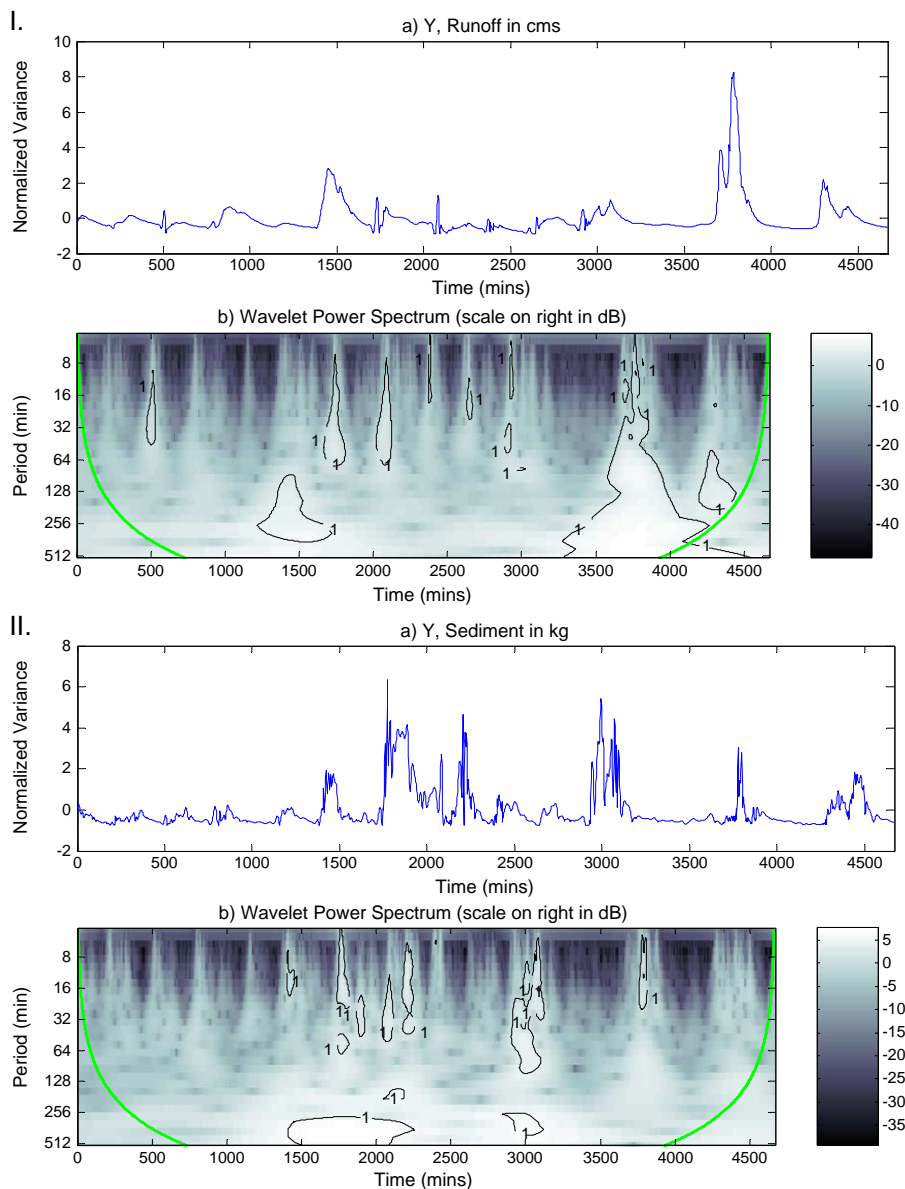
Fig. 7. Wavelet analysis for discharge and sedimentation from outlet at Y.

erosion. Incorporation of period (or inversely frequency) shifting, fragmentation, and recombination to soil loss equations (either in frequency or time space) may be viable to more realistically model erosion and transport processes in watersheds. Comparing wavelet spectra and for discharge and sedimentation measurements in upland and transported dominated watersheds (for example, in the Goodwin Creek watershed,

Mississippi) will likely provide fruitful avenues of research to examine the issues we have raised.

5. Conclusions

We analyzed the discharge and sedimentation measurements from the Riesel watershed using the complex Morlet wavelet. The major transformation processes of discharge periodicity during sedimentation are: shifting, fragmentation, and recombination. Recombination was seen to occur in discharges that were dominated by transport (routed) flows. Our approach may also provide final testing of predictive process models to capture discharge and sedimentation in large sized drainage areas.

References

Ababou, L.D., Mangin, A., 2001. Introduction of wavelet analyses to rainfall/runoffs relationship for a karstic basin: the case of Licq-Atherey karstic system (France). Groundwater 39 (4), 605–615.

Burrus, C.S., Gopinath, R.A., Guo, H., 1998. Introduction to Wavelets and Wavelet Transforms, A Primer. Prentice Hall, New Jersey. (268 pp.).

Cahill, A.T., 2002. Determination of changes in stream flow variance by means of a wavelet-based test. Water Resour. Res. 38 (6), 1-1–1-14.

Chou, C.M., Wang, R.Y., 2002. On-line estimation of unit hydrographs using the wavelet-based LMS algorithm. Hydrol. Sci. J. 47 (5), 721–738.

Jaeger, H.M., Nagel, S.R., 1992. Physics of the granular state. Science 255, 1523–1531.

Jaeger, H.M., Nagel, S.R., Behringer, R.P, 1996. The physics of granular materials. Phys. Today, 32–38 (April).

Kaiser, G., 1999. A Friendly Guide to Wavelets. Birkhäuser, Boston, MA. (300 pp.).

Knight, J.B., Jaeger, H.M., Nagel, S.R., 1993. Variation-induced size separation in granular media: the convection connection. Phys. Rev. Lett. 70 (24), 3728–3731.

Kumar, S.P., 2000. Coherent modes in multiscale variability of streamflow over the United States. Water Resour. Res. 36 (4), 1049–1067.

Kumar, P., Foufoula-Georgiou, E., 1993. A multicomponent decomposition of spatial rainfall fields: 1. Segregation of large- and small-scale features using wavelet transforms. Water Resour. Res. 29 (8), 2515–2532.

Nakken, M., 1999. Wavelet analysis of rainfall-runoff variability isolating climatic from anthropogenic patterns. Environ. Model. Softw. 14 (4), 283–295.

Nezu, I., Nakagawa, H., 1993. Turbulence in Open-Channel Flows. A.A. Balkema, Rotterdam, The Netherlands, p. 26.

Smith, L.C., Turcotte, D.L., Isacks, B.L., 1998. Stream flow characterization and feature detection using a discrete wavelet transform. Hydrol. Process. 12, 233–249.

Torrence, C., Compo, G.P., 1998. A practical guide to wavelet analysis. Bull. Am. Meteorol. Soc. 79 (1), 61–78.

Whitcher, B., Byers, S.D., Guttorp, P., Percival, D.B., 2002. Testing for homogeneity of variance in time series: long memory, wavelets, and the Nile river. Water Resour. Res. 38 (5), 1–17.

Williams, J.R., 1975. Sediment yield prediction with universal equation using runoff energy factor. RS-S-40, USDA-ARS, Washington, DC.

Yalin, M.S., 1992. River Mechanics. Pergamon Press, Oxford, UK, pp. 29–62.